Multi-scale turbulence dynamics in ohmic discharge: measured at the FT-2 tokamak and simulated by full-f gyrokinetic ELMFIRE code

S. Leerink[1], V.V. Bulanin[2], A.D. Gurchenko[3], E.Z. Gusakov[3], J.A. Heikkinen[4], A.B. Altukhov[3], L.A. Esipov[3], S.J. Janhunen[1], M.Yu. Kantor[3], T.P. Kiviniemi[1], T. Korpilo[1], D.V. Kouprienko[3], S.I. Lashkul[3] and A.V. Petrov[2]

[1]*Euratom-Tekes Association, Aalto University, Espoo, Finland*

[2]*St. Petersburg State Polytechnical University, St. Petersburg, Russia*

[3]*Ioffe Institute, St. Petersburg, Russia*

[4]*Euratom-Tekes Association, VTT, Espoo, Finland*

The complex interaction between large-scale mean E×B flows, meso-scale zonal flows and micro-scale drift turbulence, leading to anomalous transport, is an important area of experimental and theoretical research in magnetically confined plasmas.

In this paper the global electrostatic gyrokinetic (GK) particle-in-cell simulation, performed by Elmfire code [1] is for the first time validated against the turbulence and confinement data obtained in low-current ($I_p \sim 19$ kA) hydrogen ohmic discharge at FT-2 limiter tokamak ($R_0 = 55$ cm, $a = 7.9$ cm, $B_0 \sim 2.3$ T, effective collisionality: $\nu^* \sim 10$-25, main impurity: oxygen O^{+6}, $Z_{eff} \sim 3.1$, energy confinement time: 1 ms). The Elmfire code simulates the total distribution function (full-f) of drift kinetic electrons and an arbitrary selection of GK plasma ions in the region $0.25 < r/a < 1$ with a grid of 120, 150, 8 cells in radial (r), poloidal (θ), toroidal (ϕ) directions (each containing 3000 particles of each specie providing a random noise level < 1%). The 360 μs interval is computed with a time step of 30 ns. The code's solutions concerning collisions' modeling and ϕ- angular momentum conserving are described in [2, 3]. The main plasma energy losses are by heat conduction/convection and impurity radiation and ionization. Electrons are cooled according to the experimental fit of the power density of the impurity radiation and ionization. Ohmic heating is inherent by a feedback in the radially uniform loop voltage (2.25 V for the steady state) ramping up and sustaining the total current I_p. The model successfully preventing particle accumulation near the outer boundary and capturing the most prominent features of the recycling process is used. Profiles of the electron density n_e and temperature T_e (provided by Thomson scattering), the ion temperature T_i (measured at $r/a < 0.5$ by charge-exchange diagnostic and at $r/a > 0.6$ by visible light spectroscopy) used as the simulation input and steady state profiles (for the

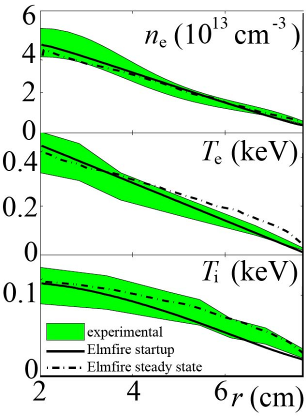

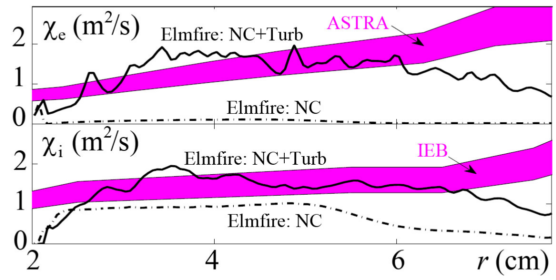

Fig. 1. Radial profiles. NC – the neoclassical like stage of simulation (0..180 μs) without turbulence modes with ϕ - mode number n ≠ 0, Turb - the stage (180..360 μs) with a turbulence switched on.

turbulent stage of the simulation) are shown on Fig. 1. T_i for O^{+6} and H^+ were assumed to be equal. An overall good agreement between the numerical expectations and the experimental estimations of the effective electron and ion heat conductivity obtained from the primary experimental profiles using ASTRA modeling [4] for the former one and energy balance in the ion channel (IEB) for the latter were achieved (Fig. 1) with exceptions at the outer boundary. The partial agreement of the full-f modeling results achieved at the macro-level was strengthened at the micro and intermediate turbulent scale level by comparisons to Doppler Reflectometry (DR) [5] and Doppler Enhanced Scattering (ES) [5, 6] microwave diagnostic measurements of fluctuation spectra and perpendicular rotation. Both diagnostics utilize electromagnetic wave back scattering (BS) (for DR: 26-37 GHz, *O*-mode in the cutoff vicinity: $r/a \sim 0.8$-0.9, with resolution $\delta r \sim 0.5$ cm; for ES: 54-66 GHz, *X*-mode at the upper hybrid resonance (UHR) layer: $r/a \sim 0.65$-0.87, with $\delta r \sim 0.1$ cm) off low frequency small-scale density fluctuations with θ - wave numbers for DR: $k_\theta \sim 3$-5 cm^{-1}; for ES: 15-30 cm^{-1}.

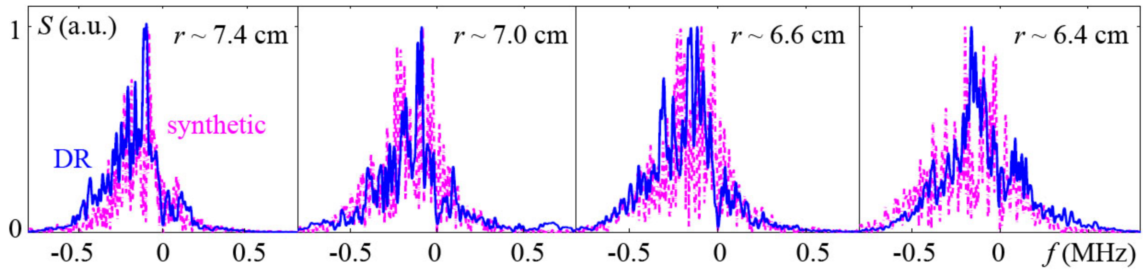

Fig. 2. Spectra comparison: DR (blue) and synthesized from Elmfire simulations with impurities (magenta).

Comparisons between the experimental DR frequency (f) spectra at several r-positions and spectra reconstructed using the density fluctuations $\delta n(r,\theta,t)$ simulated by the code [7] through the relation $S(f) = \int_{-\infty}^{\infty}\int_0^{2\pi}\int_0^{r} W(r,\theta)\delta n(r,\theta,t)\exp(-i2\pi ft) r dr d\theta dt$ where $W(r,\theta)$ is a complex DR weighting function, used to select the spatial and wave number (k) range of turbulence, are shown in Fig. 2, where the statistical averages on the saturated nonlinear state are performed over 64 μs to obtain similar statistics. Micro-scale turbulence f-spectra measured by the DR diagnostic can be reconstructed and the f-shift, the width and even the shape of the experimental spectra are well reproduced by the synthetic diagnostic indicating

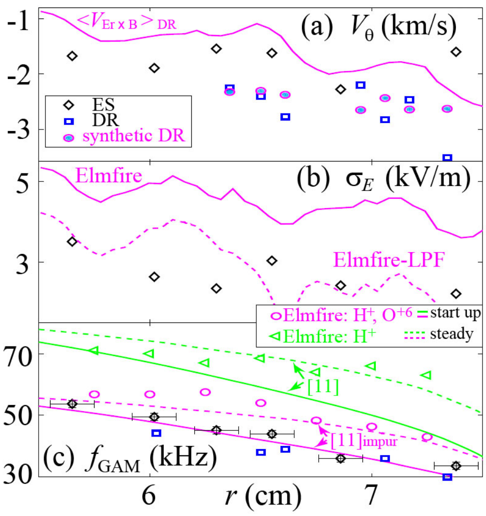

Fig. 3. Radial profiles of the V_θ (a), E_r standard deviation (b), the dominant frequency in the $E_r(t)$ spectrum (c).

comparable rotation and spreading of the selected turbulent density fluctuations. The fluctuation poloidal rotation velocity V_θ profile obtained from the mean *f*-shift of the experimental spectra (Fig. 3a) is very close to that obtained from the synthetic spectra. However it is slightly higher than the computed $V_{Er \times B}$ plasma rotation profile averaged over the DR domain (magenta curve). This difference should be attributed to the fluctuation phase velocity, which appears to be smaller than the plasma rotation velocity. The V_θ of drift wave fluctuations responsible for BS in the UHR obtained from the mean value of the ES f_D appears to be close to that given by DR, indicating similar V_θ for density fluctuations with different k_θ.

As usual in scattering experiments [8, 9], the spectral width of the DR spectrum is larger (a factor of 2) than the value, prescribed by the *k*-resolution technique. This difference is explained, in substantial part, by fast and strong variation of the E_r observed in modeling (Fig. 4a). These giant E_r oscillations at a frequency of 30-50 kHz are attributed to the geodesic acoustic mode (GAM). Such an attribution is supported by DR and ES measurements revealing similar oscillations in the V_θ meso-scale dynamics. By applying the sliding Fourier Transform (FT) procedure (or the δ-phase method [10]) to quadrature BS signals one can generate $f_D(t)$ time sequences which can then be Fourier analyzed to give the E_r spectrum and reveal the GAM like spectral lines. In Fig. 3c the dominant E_r oscillation frequency dependence on the *r*-position obtained by Elmfire simulations with (magenta) and without (green) impurities and BS measurements are compared with the analytical prediction [11] for the GAM frequency (solid and dashed curves) in which the role of impurities is accounted for $n_i = 0.07n_e$. When the O^{+6} component is included in the simulations a much better match to the analytical estimation obtained for relaxed profiles as well as to the ES and DR measurements is found. Due to insufficient *r*-resolution the contrast of the GAM spectral peak is not high (< 2) for the DR measurements complicating the V_θ meso-scale dynamics investigation against the background wideband

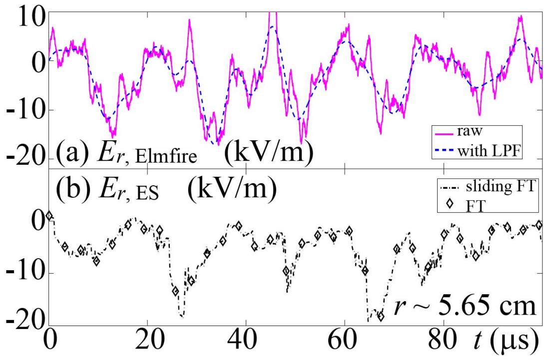

Fig. 4. E_r time traces.

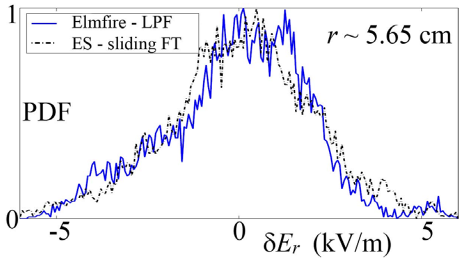

Fig. 5. PDFs of the E_r fluctuations.

noise f_D oscillations. Therefore the V_θ dynamics was studied in more detail using the ES diagnostic possessing a much better δr and higher GAM contrast (~ 4). The $E_r(t)$ time trace obtained with the ES technique (Fig. 4b) was constructed from BS spectra with a FT window of 64 points and a sampling period of 50 ns, corresponding to a Nyquist frequency of $f_N = 156.25$ kHz. For one on one comparison between the simulated and experimental E_r fluctuations, frequencies above the f_N are removed from the simulated $E_r(t)$ by a low pass filter (LPF) (the dotted line in Fig. 4a). The probability distribution functions (PDFs) of $\delta E_r(t) = E_r(t) - < E_r >$, where $< E_r >$ is the time averaged mean (at $r \sim 5.65$ cm) are shown to be similar and well approximated by normal law (Fig. 5). At various r-positions a good quantitative agreement is found between the experimental and simulated standard deviations (σ_E) of the δE_r PDFs when LPF is applied (Fig. 3b).

Conclusion.

Summarizing, direct measurements of micro, meso, and macro-scale transport phenomena in the FT-2 tokamak are shown to be quantitatively reproduced by global full-f nonlinear GK simulation predictions with Elmfire code. A detailed agreement with mean equilibrium E×B flows, oscillating meso-scale zonal flows and turbulence spectra observed by a set of sophisticated microwave BS techniques as well as a good fit of the thermal diffusivity data are demonstrated. A clear influence of the impurity ions on the fluctuating E_r is observed.

This work is supported by the grants 122435 and 134977 of the Academy of Finland, RFBR grant 10-02-00631, the Russian Academy program 12, the RF Government grant 11.G34.31.0041, the EFDA Topical Group Activities and is part of the national Tekes work program. The High Level Support Team and the CSC IT Center for Science Ltd. CSC, DEISA, PRACE and HPC-FF are acknowledged for the allocation of manpower and computational resources for this work.

[1] J.A. Heikkinen et al., J. Comp. Phys. 227, 5582 (2008)
[2] T. Takizuka et al., J. Comput. Phys. 25, 205 (1977)
[3] J.A. Heikkinen et al., Comput. Phys. Commun. 183, 1719 (2012)
[4] G.V. Pereverzev and P.N. Yushmanov, Preprint IPP 5/98 Garching (2002)
[5] E.Z. Gusakov et al., Plasma Phys. Control. Fusion 48, B443 (2006)
[6] A.D. Gurchenko et al., Plasma Phys. Control. Fusion 52, 035010 (2010)
[7] S. Leerink et al., Contrib. Plasma Phys. 50, 242 (2010)
[8] P. Hennequin et al., Plasma Phys. Control. Fusion 46, B121 (2004)
[9] A.D. Gurchenko et al., Nucl. Fusion 47, 245 (2007)
[10] G.D. Conway et al., Plasma Phys. Control. Fusion 47, 1165 (2005)
[11] W. Guo et al., Phys. Plasmas 17, 112510 (2010)